Amelioration of Saline-Alkali Soil with Rice Straw Biochar: Impacts on Aggregate Composition, Organic Carbon, and Microbial Biomass

Fengli Cheng,[a] Guixiang Quan,[a,b] Hui Wang,[a,b] Liqiang Cui,[a,b] Dezhi Yan,[a] and Jinlong Yan [a,b,]*

* *Corresponding author. yjlyt@ycit.cn; yjlyt4788@126.com; (+86 13851182530)*

DOI: 10.15376/biores.21.3.6846-6865

GRAPHICAL ABSTRACT

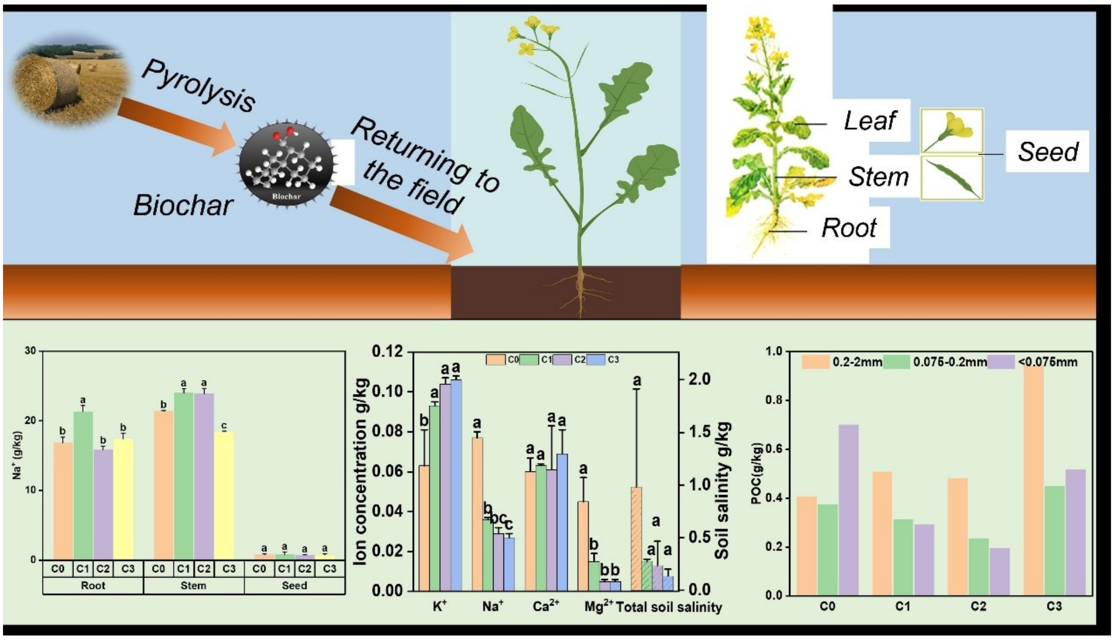

Amelioration of Saline-Alkali Soil with Rice Straw Biochar: Impacts on Aggregate Composition, Organic Carbon, and Microbial Biomass

Fengli Cheng,[a] Guixiang Quan,[a,b] Hui Wang,[a,b] Liqiang Cui,[a,b] Dezhi Yan,[a] and Jinlong Yan [a,b,]*

Against the backdrop of increasingly severe global food security challenges and constraints on arable land, the remediation and efficient utilization of saline-alkali land has become a critical issue. While biochar shows significant potential for the remediation of saline-alkali soil, the mechanisms involved at the aggregate scale remain unclear. This study investigated the effects of application levels (0%, 1%, 2% and 5%) of rice straw biochar on the physicochemical properties, aggregate organic carbon, and mineralization in saline-alkali soil. The results indicated that biochar application significantly decreased soil pH and the concentrations of Na^+ and Mg^{2+} ions, while increasing the levels of K^+ ions and exchangeable Ca^{2+} ions. These changes effectively improved the soil's ionic environment and fertility, thereby promoting the growth of rapeseed seedlings. Biochar also enhanced microbial biomass carbon and activity, facilitating organic carbon transformation and stabilization. Furthermore, an appropriate amount of biochar significantly increased the proportion of 0.075 to 0.2 mm and 3 to 2 mm aggregates, thereby promoting the aggregation of microaggregates into macroaggregates. These findings clarify how biochar enhances the stability of aggregate organic carbon by improving soil structure, regulating ion composition, and modulating microbial activity. This provides a theoretical basis for the remediation of saline-alkali soil.

DOI: 10.15376/biores.21.3.6846-6865

Keywords: Saline-alkali soil; Biochar; Salinity; Aggregate; Microbial biomass

Contact information: a: School of Environmental Science and Engineering, Yancheng Institute of Technology, Yancheng 224051, China; b: Jiangsu Engineering Research Center of Biomass Waste Pyrolytic Carbonization & Application, Yancheng 224051, China;
** Corresponding author. yjlyt@ycit.cn; yjlyt4788@126.com; (+86 13851182530)*

INTRODUCTION

Soil plays a pivotal role in maintaining agricultural productivity and global food security by facilitating nutrient cycling, root anchorage, and water retention. Approximately 3.93 million hectares of arable land are currently in use in China. Of this, 67.68% is grassland, 8.11% is sandy land, 20.68% is saline-alkali land, and 3.53% is bare land (Chen *et al.* 2024). Among these, saline-alkali soil is one of the most widely distributed types of low-yield land worldwide, across in the eastern coastal regions and northeastern regions and western arid and central semi-arid regions of China. However, its high salinity, elevated pH, and poor physical structure severely limit agricultural output and ecological functioning (Haj-Amor *et al.* 2022; Wu *et al.* 2024; Ait Lahssaine *et al.* 2025; Lei *et al.* 2025). Against the backdrop of increasingly limited arable land resources and continuously growing worldwide demand for food, it has become crucial to improve and utilize saline-alkali land in order to ensure food security and promote ecologically sustainable development (Li *et al.* 2025a). Effective remediation strategies can alleviate land resource pressures and support regional economic growth, making saline-alkali soil restoration a major research focus. Among various measures for saline-alkali land improvement, biochar has become a promising soil amendment due to its multiple functional benefits (Cui *et al.* 2022) .

Biochar has widespread application in soil remediation. Its unique chemical, physical, and biological properties, such as its high organic carbon content, low bulk density, and large specific surface area, are reasons for its broad applicability (Zhao *et al.* 2023; Wang *et al.* 2024a). A five-year field study revealed that wheat straw-derived biochar significantly improved paddy soil properties (Cui *et al.* 2016). Similarly, a corn pot experiment, adding 30 g/kg of biochar increased soil organic carbon by 20.0%, available phosphorus by 39.5%, and available potassium by 53.5%, compared with control soil (Zhu *et al.* 2022).

Biochar also influenced the soil microbial communities after applied in the soil (Zou *et al.* 2022; Wang *et al.* 2024b; Zhang *et al.* 2024b). A one-year laboratory incubation study demonstrated that biochar application significantly enhanced microbial proliferation and activity, which in turn accelerated the oxidative aging and dissolution of biochar (Quan *et al.* 2020b). Soil enzymes, as functional products of microbial metabolism, are highly coupled with microbial proliferation and activity changes, jointly driving soil material transformation, energy flow, and nutrient cycling processes. Biochar, by improving the soil microenvironment and enhancing organic carbon supply, not only promotes substantial microbial proliferation, but it also significantly increases the activity of key soil enzymes such as β-glucosidase and leucine aminopeptidase. This strengthens the coupling of soil carbon, nitrogen, and phosphorus cycles, thereby synergistically promoting the structural improvement and fertility enhancement of saline-alkali soils. Biochar has positive effects on soil properties and bacterial community, which further positively regulate soil C, N, and P acquiring enzymes. Key factors driving enzyme variations include available P, SOC, available K, available N, total K, and total N, as well as soil bacterial community composition and diversity (Wang *et al.* 2025a).

Previous studies have shown that biochar amendment significantly enhances saline-alkali soil properties by improving moisture retention and increasing organic carbon, available potassium, and cation exchange capacity (Quan *et al.* 2020a). Schurkamp *et al.* (2024) also found that biochar has great potential to reduce soil salinity, enhance aggregate stability, and improve crop yields. As key indicators of soil fertility, the formation and stability of aggregates directly affect physical, chemical, and biological soil properties (Abiven *et al.* 2009; Zhang *et al.* 2025b). Under saline-alkaline conditions, aggregates are particularly vulnerable to degradation due to high salinity and/or strong alkalinity, leading to structural deterioration and functional decline of soils. This process ultimately imposes severe constraints on agricultural productivity (Li *et al.* 2025b). Because of the special regional characteristics of the biochar microdomains, biochar releases small molecules that change the morphology of organic matter, thereby indirectly altering the composition of soil organic matter and the structure of aggregates. Consequently, biochar enhances aggregate stability and improves overall soil structure (Lu *et al.* 2014). The utilization of biochar for the amelioration and remediation of saline-alkali soils has garnered substantial academic interest (Wu *et al.* 2025; Xie *et al.* 2025; Yang *et al.* 2025b).

Despite this promise, the mechanisms governing biochar's interaction with soil salinity remain poorly understood. In particular, limited information is available regarding biochar amendment effects on: (1) soil fertility and salinity; (2) dose-dependent crop responses across different growth stages; and (3) the formation of soil aggregates and their associated microbial communities. To address these issues, a pot experiment was conducted to systematically evaluate the impact of biochar on rapeseed growth, soil fertility, salinity dynamics, aggregate distribution, and microbial community composition. The study investigated how biochar application levels impacted soil quality and plant productivity in saline-alkali environments, thereby supporting the development of targeted bioremediation strategies.

EXPERIMENTAL

Field and Soil Sampling

Saline-alkali soil was collected from agricultural fields at a 0 to 20 cm depth in Yandong Town, Tinghu District, Yancheng City, Jiangsu Province, China (33°34′12″N, 120°23′24″E). This area, located near the Yellow Sea, has an average temperature of 13.7 to 14.4 °C and an annual rainfall of 900 to 1,067 mm. Soils were subjected to one week of air-drying under sunlight exposure before the removal of visible impurities (*e.g.*, stones and root debris). Biochar made from rice straw by pyrolysis at 450 °C was purchased from Qinfeng Zhongcheng Biomass New Materials (Nanjing) Co., Ltd. The characteristics of the soil and biochar are exhibited in Table S1. The soil has a high pH level (8.0), a low organic carbon content (3.53 g/kg), and is infertile and highly saline (1.52 g/kg), which can be classified as a saline-alkali soil.

Pot Experiment Design

The pot experiment was conducted at Yancheng Institute of Technology (33°24′20″N, 120°10′13″E; altitude: 10.3 m a.s.l.), Jiangsu Province, China. Before conducting the pot experiments, soil fertility was enhanced by applying a compound fertilizer containing 15% nitrogen, phosphorus, and potassium at a level of 0.75 t/ha and thoroughly mixing it into the soil. The mixed soil was placed into a 40 x 50 cm PVC bucket. This study employed four experimental treatments: no biochar (C0), 1% biochar (C1), 2% biochar (C2), and 5% biochar (C3), each with three replicates. On 29 November 2024, three Gold No. 9 rapeseed seedlings were transplanted into each pot.

Soil Collection, Pretreatment, Physicochemical Analysis, and Aggregate Classification

After collection, the soil samples were air-dried and sieved through 10-, 18-, and 110-mesh sieves for later use. From from the 10-mesh sieve, 10 g of soil was removed, and 25 mL of deionized water was added. The mixture was shaken for 2 min and left to settle for 30 min, and then the soil's physicochemical properties were determined using the different method (Liu *et al.* 2024). The pH was measured (pHS-3C pH meter). Total phosphorus (TP) and total potassium (TK) were determined using the alkali fusion method. Briefly, 0.2 g of soil (100 mesh) was placed into a 30 mL nickel crucible, and a few drops of anhydrous ethanol were added to moisten the sample. The sample was covered with 2 g of NaOH and heated in a muffle furnace to produce an alkali solution. The sample was measured using a UV-visible spectrophotometer and an atomic absorption spectrophotometer. Total organic carbon (TOC) and Total soil nitrogen (TN) was determined. The supernatant was used for atomic absorption spectrophotometry to determine the concentrations of K^+, Na^+, Ca^{2+}, and Mg^{2+}.

Methods used to study soil aggregate stability include dry and wet sieving procedures. The differential swelling of clay upon wetting may contribute to aggregate destruction. The dry effect also depends on the swelling behavior and thus on the mineralogy of the clay minerals. The dry sieving procedures was significantly influenced of human operation. On the microaggregate scale, wet sieving procedures were mainly influenced by water, since they resembled conditions found in nature (Abiven *et al.* 2009). So, original soil samples were classified using the wet sieve method for soil aggregates. The samples were divided into the following categories: > 2.0 mm, 2.0 to 0.2 mm, 0.2 to 0.075 mm, and <0.075 mm. The specific method was as follows: 10 g of the original soil sample was placed in a sieve with aperture sizes of 2.0 mm, 0.2 mm, or 0.075 mm. The soil sample was submerged in water for 5 min and oscillated at 30 rpm for a further 5 min. The samples were removed and left to stand. The soil from each sieve was washed into an aluminium box of known mass and dried at 60 °C until it reached a constant weight (Jiang *et al.* 2025). The percentage mass of soil aggregates at each level was calculated, as well as weight diameter (*e.g.*, MWD), and geometric mean diameter (*e.g.*, GMD), as follows (Yuan *et al.* 2025b),

$$MWD = \sum_{i=1}^{n} W_i \overline{X_i} \quad (1)$$

$$GMD = Exp\left(\sum_{i=1}^{n} W_i \ln \overline{X_i}\right) \quad (2)$$

where X_i is the average diameter (mm) of each size of soil aggregate, and W_i is the weight percentage of each size of soil aggregate.

The chloroform fumigation method was used to determine the microbial biomass in soil aggregates of different particle sizes (Ju *et al.* 2024). Fresh soil samples were equally divided into fumigated and control groups. The fumigated group were placed in a vacuum desiccator containing 25 mL of ethanol-free chloroform ($CHCl_3$) and fumigated for 24 h at a constant temperature of 25 °C, followed by vacuum to completely remove residual chloroform. Then, a 0.5 mol/L K_2SO_4 solution (solid: liquid=1:4) was added, and the mixture was oscillated at 200 rpm for 30 min at 25 °C. The extract was filtered by 0.45 μm membrane. The microbial biomass carbon (MBC) was determined *via* the potassium dichromate oxidation–external method. The microbial biomass nitrogen (MBN) was measured *via* the semimicroscopic Kjeldahl method. From the bolting stage onward, rapeseed growth parameters, including plant height and chlorophyll content (Zamani *et al.* 2025), were measured monthly. Briefly for chlorophyll extraction, the leaf tissue was pulverized and resuspended in 200 μL 25 m mol/L sodium phosphate buffer (pH 7) and 0.8 mL 80% (v/v) acetone. Samples were then incubated at room temperature in the dark for 1 h with gentle shaking and centrifuged for 10 min at 3000 g. The absorbance (*D*) at 645 and 663 nm was measured. The total chlorophyll content was then calculated with the following formula: $\text{chlorophyll}_{\text{Total}} = 20.2 \times D_{645} + 8.02 \times D_{663}$.

The soil physicochemical properties were also detected with different methods (Bao 2008). Soil pH was measured using a pH meter (PHS-3C, Shanghai, China) at a soil to water ratio of 1: 2.5 (m/v). The total soil organic carbon content was quantified using the dichromate oxidation method. Soil water content was determined gravimetrically by weight difference before and after at least six hours of oven drying at 105 ºC. The soil cations (Ca, Mg, K, Na) were determined *via* atomic absorption spectrometry (AAS; TAS-986, Persee, China)

Total nitrogen (total N) was determined using the semi micro-Kjeldahl procedure with Kjeldahl determination apparatus (UDK139, VELP, Italy). Total phosphorus (total P) was measured using the NaOH fusion–Mo–Sb anti-spectrophotometric method with P concentration determined *via* a spectrophotometer (TU-1901, Persee, China). And, total potassium (total K) was determined via NaOH fusion, with K concentration determined using AAS.

The particulate organic carbon (POC) and mineral-associated organic carbon (MAOC) were determined as follows: weigh out 5.00 g of soil and place it in a 50 mL centrifuge tube. Add 25 mL of a 5 g/L sodium hexametaphosphate solution, then oscillate at 180 r/min for 18 h. Pass the mixture through a 270-mesh sieve. The fraction retained on the sieve represents particulate organic carbon (POC), while the remaining fraction constitutes mineral-associated organic carbon (MAOC). All POC and MAOC specimens were dried in an oven at 60 °C until they reached a stable mass, after which they were weighed and stored (Yuan *et al*, 2025a).

Analysis of Plant Samples

Once the oilseed rape matured, the number of first-grade branches and stem thickness were measured, as well as the number of angiosperms. Then, 5 to 10 g of oilseed rape seeds was randomly selected to measure yield-related indexes such as seed moisture content and thousand-grain weight. Finally, the physicochemical properties of the seeds, such as oilseed rape proteins and oil content, were measured using randomly selected oilseed rape seeds. Dried rapeseed grains were passed through a 40-mesh sieve. The Kjeldahl method (GB 5009.5-2016) (Defaix *et al.* 2019) was used to determine the protein content, and the Soxhlet extraction method (GB/T 14772-2008) (Wang *et al.* 2022) was used to determine the oil content.

DNA Extraction and Sequencing of Bacterial 16S rRNA Gene

Changes in soil microbial communities were investigated using 16S rRNA bacterial sequencing technology. Samples were collected from four treatment groups (C0, C1, C2, and C3) following the harvest of rapeseed. The samples were sent to Jisihuiyuan (Nanjing, China) for analysis. This study evaluated the effects of different rates of biochar application on the relative abundance of soil microorganisms, particularly those associated with soil salinity.

Data Analysis

The experimental results for each treatment are presented as mean values ± standard deviation (SD). Statistical analyses of the fundamental physicochemical properties and salt content of the saline-alkali soil were performed using one-way ANOVA in SPSS 26.0 (IBM Corp., USA), with post-hoc Duncan's multiple range test at a significance level of $p < 0.05$. Data visualization was conducted using Origin 2024 software (OriginLab Corporation, USA).

RESULTS AND DISCUSSION

Effects of Biochar on Soil Physical and Chemical Properties

Figure 1 shows the effect of biochar application on the physicochemical properties of saline-alkali soil over time. Soil pH initially increased and then decreased after biochar application, compared to the control. Biochar-induced pH dynamics exhibited temporal variability (Feng *et al.* 2024). The initial rise in pH, attributed to the alkaline ash components of biochar, was followed by a subsequent decline in later stages. This pattern is consistent with a previous study showing that applying biochar alone or in combination with nitrogen fertilizer reduced soil pH (Zhang *et al.* 2024b). The TP content remained above that of the control group throughout the study, though there was minimal overall variation, which is consistent with previous studies (Yuan *et al.* 2025a). Relatively speaking, the TOC, TN, and TK content of all biochar-treated soils was significantly higher than that of C0. As the time since biochar application increased, these contents gradually decreased from initial levels. TOC and TN exhibited greater variability, with C3 decreasing by 33.8% and 20.0%, respectively. As a carbon-rich solid waste material, biochar incorporation markedly increased TOC content (Wang *et al.* 2025b).

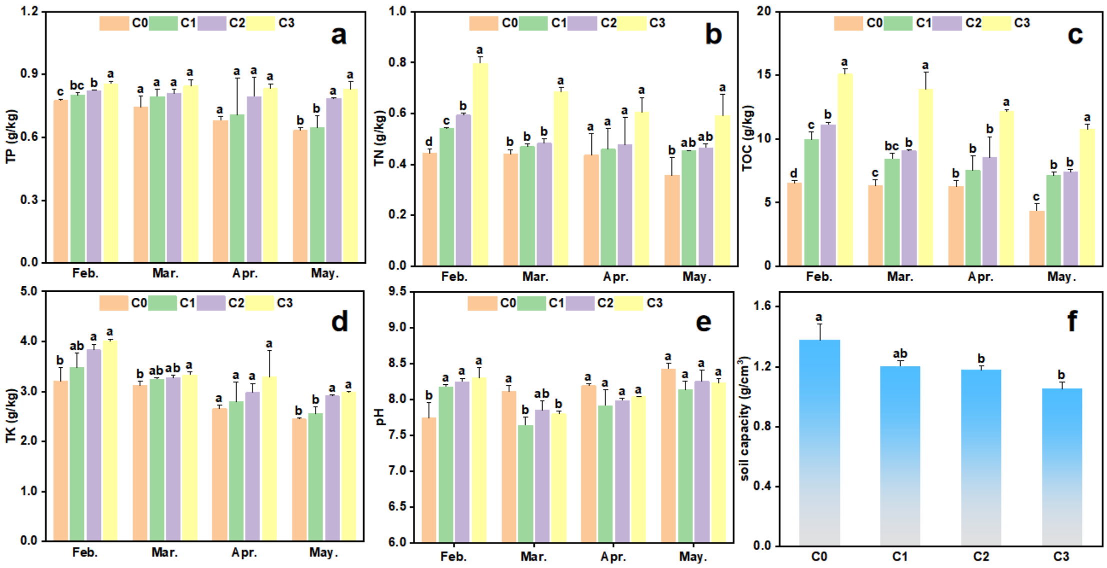

Fig. 1. Temporal variations of soil fertility indicators under differential biochar application rates. C0: control (no biochar) C1: 1% biochar (w/w) C2: 2% biochar (w/w) C3: 5% biochar (w/w). a: total P, b: total N, c: TOC, d: total K, d: pH, f: soil bulk density. Different lowercase letters indicate statistically significant differences among treatments (*p* < 0.05 by Tukey's HSD test).

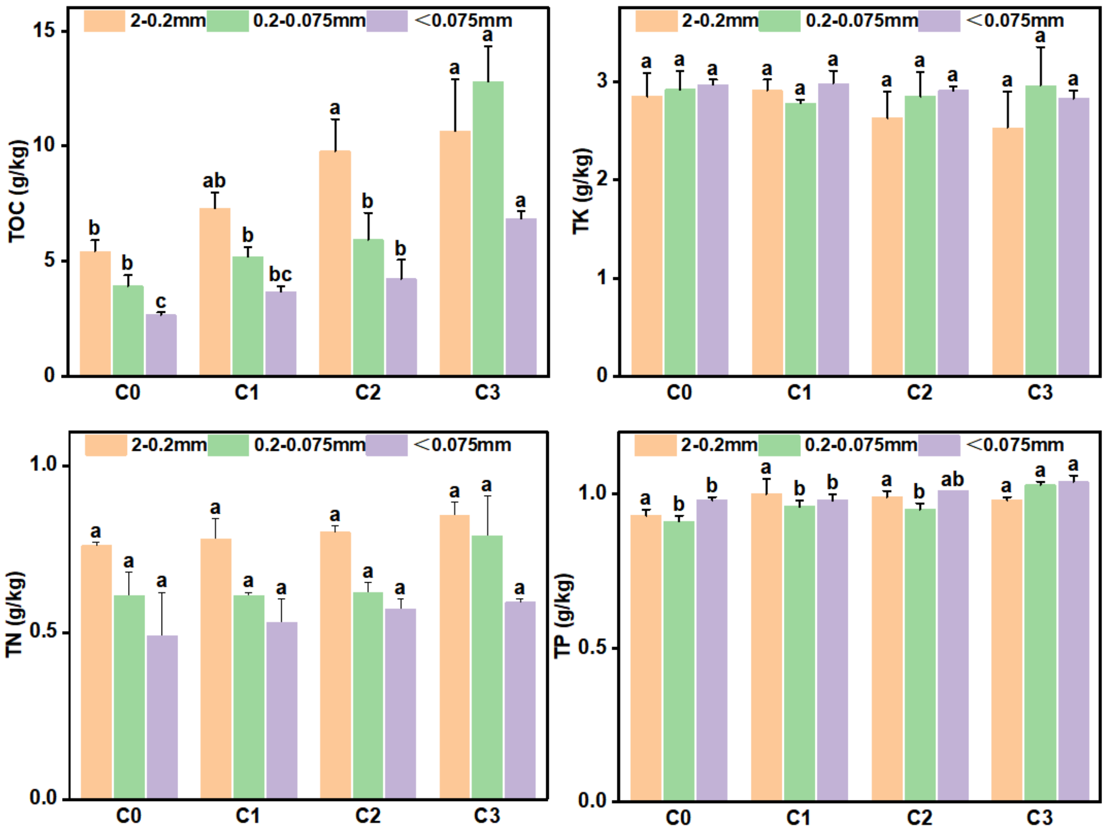

Fig. 2. Changes in fundamental physicochemical properties of soil aggregates under different biochar treatments: total organic carbon (TOC), total nitrogen (TN), total phosphorus (TP), and total potassium (TK) across aggregate size fractions (2-0.2 mm, 0.2-0.075 mm, and <0.075 mm). Different lowercase letters indicate statistically significant differences among treatments (p < 0.05 by Tukey's HSD test).

Concurrently, the inherent nitrogen in biochar led to elevated TN levels, showing a positive correlation with application rate. Biochar amendment also influenced soil bulk density (BD) and field water-holding capacity (WHC) after the harvest of crops. Results indicated a downward trend in BD, with reductions of 13.0%, 14.5% and 23.9% in the

C1, C2, and C3 treatments compared to the control. Conversely, WHC increased by 30.4%, 35.4%, and 41.5% respectively.

Changes in TOC, TK, TN, and TP within soil aggregates of different particle sizes were further investigated. As shown in Fig. 2, applying biochar significantly increased the total organic carbon (TOC) content of soil aggregates. There was a particularly pronounced enrichment effect in large aggregates (2 to 0.2 mm) and microaggregates (0.2 to 0.075 mm). The TOC content in large aggregates reached 10.65 g/kg under the C3 treatment, which is a 96% increase compared to the control (5.44 g/kg). Meanwhile, the TOC content in microaggregates (0.2 to 0.075 mm) was 3.26 times that of the control. These results suggest that, on the primary level, biochar enters microaggregates directly in the form of fine particles. On the secondary level, it may also promote the migration and accumulation of carbon in macroaggregates by enhancing aggregate formation and stability. However, no significant changes in TK, TP, or TN content were observed following biochar application across all particle size fractions ($p>0.05$).

A recent meta-analysis concluded that biochar application consistently enhances the sequestration of organic carbon and nitrogen within soil aggregates (Yuan, X. *et al.* 2025b). While the findings align with this general trend for TOC, which showed a consistent increase across aggregate fractions, the response of aggregate-associated TN was less pronounced, exhibiting only a non-significant increase. This discrepancy could be attributed to biochar-enhanced denitrification during the wet sieving process, potentially leading to nitrogen loss (Yuan *et al.* 2019).

Effect of Biochar on Salts of Soil

The temporal dynamics of cationic salt ions (K^+, Na^+, Ca^{2+}, Mg^{2+}) in saline-alkali soil under different biochar treatments are shown in Fig. 3A. Biochar application initially led to a significant reduction in soil total salt content; however, this desalination efficacy diminished over time. The application of biochar considerably increased the potassium (K^+) content of the soil, while reducing the sodium (Na^+) concentration. Among all treatments, the C3 regimen demonstrated the most pronounced effect, achieving the highest K^+ accumulation (0.454 g/kg) in February. Although not statistically significant, a numerical increase in calcium ion (Ca^{2+}) levels was noted across the biochar treatments compared to the crop-control. K^+, Na^+, Ca^{2+}, and Mg^{2+} are key components of soil salinity, and their excessive accumulation beyond specific thresholds can adversely affect plant growth (Haj-Amor *et al.* 2022).

The impact of biochar on soil ion dynamics is variable and context-dependent. For instance, Duan *et al.* (2021) reported that biochar effectively adsorbed Na^+ in highly saline-alkali soils while simultaneously releasing K^+ and Ca^{2+}. Similarly, dos Santos *et al.* (2022) observed that the application of biochar leads to an increase in soil K^+ content due to its inherently high K^+ concentration. Pearson correlation analysis was conducted to investigate the relationship between biochar application rates, soil salinity, and associated ion concentrations (Fig. 3B). The results showed a significant positive correlation between the amount of biochar applied and the concentration of potassium ions in the soil, seeds, and stems of rapeseed, and soil and leaves. There was also a negative correlation between the amount of biochar applied and salinity and sodium ions. In terms of salinity mitigation, the high adsorption capacity of biochar effectively alleviated salt stress, supporting conclusions from the existing literature (Yue *et al.* 2023).

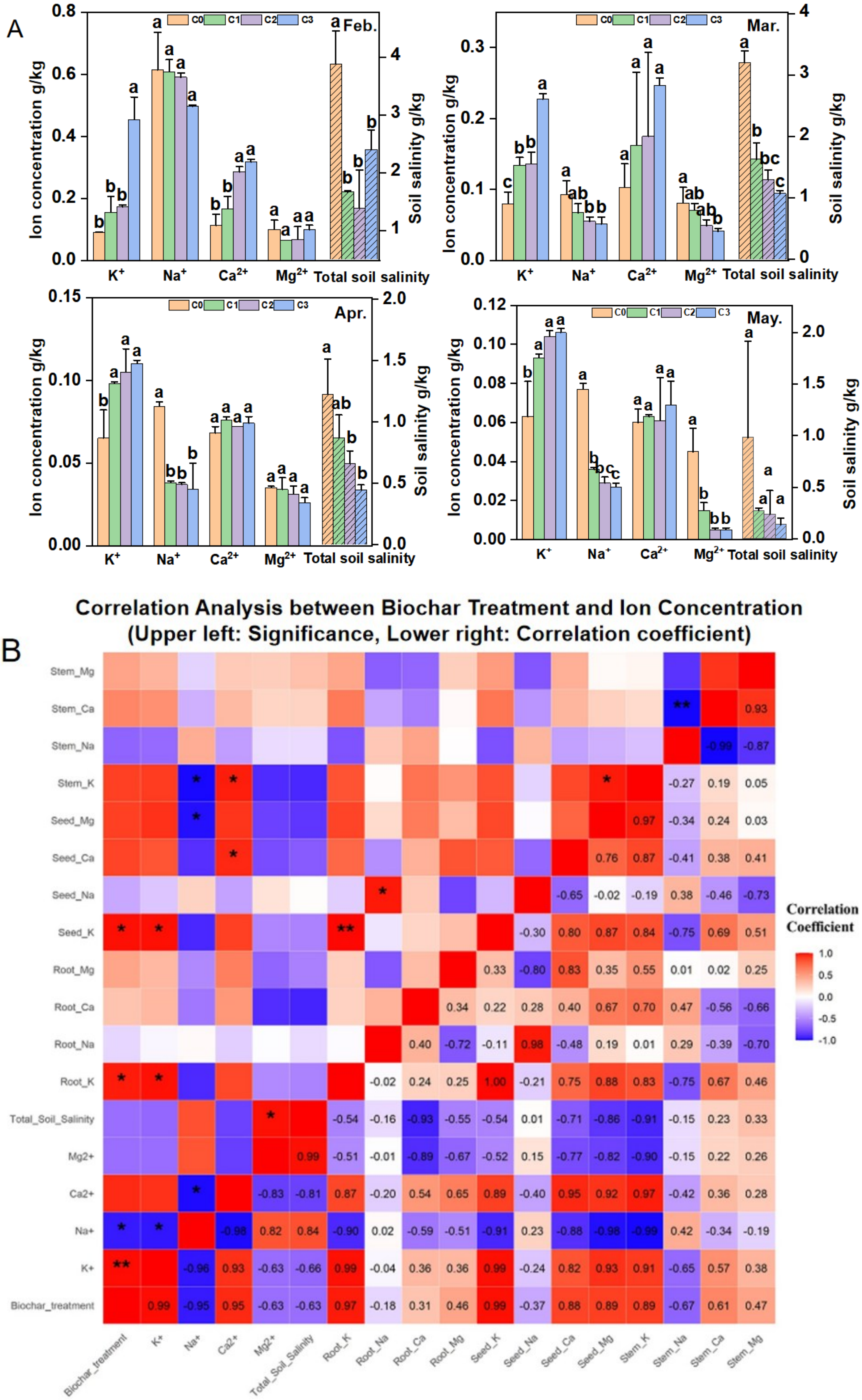

Fig. 3. Changes in cationic salt ions of saline soils under different biochar treatments over time (A) and correlation analysis (B). Different lowercase letters indicate statistically significant differences among treatments (Note: * p<0.0.05; ** p<0.01).

Effect of Biochar on the Growth of Oilseed Rape

This study systematically evaluated the effects of applying biochar on the growth, development, and yield components of rapeseed, as well as its seed quality. The results indicate that the effects of biochar differed depending on the growth stage and indicator, with significant dose-dependent and complex responses observed. During the vegetative growth stage, as illustrated in Fig. S1, biochar treatments consistently promoted growth. From the bolting stage onwards, the plant height and leaf number of all biochar treatment groups (C1 to C3) significantly exceeded those of the control group (C0). Concurrently, leaf chlorophyll content positively correlated with the application rate of biochar, peaking at 2.060 mg/g in the C2 treatment group in March. Overall, these findings demonstrate that biochar effectively enhanced rapeseed vegetative growth. Regarding yield and quality, however, biochar's effects were more complex (Table 1). Biochar treatments had positive effects on yield components: the C2 treatment increased 1000-seed weight by 3.93% compared to the control, and all treatments significantly increased stem diameter. However, for seed quality, protein content decreased in all treatments, with the largest reduction (9.37%) observed in the C3 treatment. Although no significant differences were observed overall between treatments for seed oil content, the C1 treatment recorded the highest value (42.0 ± 2.8%). Notably, as the application level increased from C1 to C2 and C3, yield decreased, and seed oil content showed a significant downward trend.

Table 1. Indicators of Oilseed Rape Growth under Different Biochar Treatments

	PBN	MSD (cm)	SMC (%)	SN	MCS (%)	TSW (g)	TSY (g)	SPC (g/100g)	OC (%)
C0	9±1.94a	4.77±1.00b	37.4±0.03a	927±86.3a	54.0±0.01a	4.51±0.29a	69.58±1.24a	27.27±0.59a	41.0%±1.4%a
C1	9±2.48a	5.80±1.49ab	34.1±0.03a	965±287.1a	56.5±0.01a	4.50±0.20a	72.19±2.87a	26.34±0.13ab	42.0%±2.8%a
C2	9±1.47a	6.36±0.69a	37.3±0.11a	846±232.6a	57.6±0.02a	4.68±0.29a	68.88±3.16a	25.34±0.62bc	31.0%±1.4%b
C3	10±0.98a	5.94±0.98ab	39.9±0.02a	901±1.4a	57.2±0.04a	4.23±0.20a	68.76±12.07a	24.71±0.20c	28.0%±2.8%b

Notes: PBN: Primary branch number, MSD: Mean stem diameter, SMC: Seed moisture content, SN: Silique number, MCS: Moisture content of siliques. TSW: Thousand-seed weight, TSY: Total seed yield, SPC: Seed protein content, OC: Oil content. Different lowercase letters indicate statistically significant differences among treatments ($p < 0.05$ by Tukey's HSD test).

The promotion of crop growth by biochar is primarily attributed to its ability to improve soil physicochemical properties, optimize the morphological development of plant roots, stems, and leaves, and lay the foundation for flower and fruit development (Simiele *et al.* 2022). This study found that the biochar-treated groups showed significant advantages from as early as the vegetative stage (from rosette to initial flowering), which supports this mechanism. However, the ultimate effects of biochar are subject to complex regulation by soil type, climatic conditions, and application level, which introduces uncertainty in its practical application. The literature reports divergent conclusions across studies. For example, Jeffery *et al.* (2011) found no significant yield increase ($p > 0.05$) at moderate application levels (*e.g.* 40 and 65 t/ha), while another study achieved a 36.02% yield increase in rapeseed by applying 40 t/ha of biochar to red soil (Liu *et al.* 2014). The results of the present study reflect this complexity: only low application levels (C1) had neutral or slightly positive effects on yield and oil content, whereas medium-to-high levels (C2 and C3) had inhibitory effects. This confirms the existence of an optimal application level window for biochar, with its effects varying according to specific environmental conditions (Lehmann *et al.* 2015).

Deeper insights into the physiological mechanisms underlying the observed growth and yield responses were gained by analyzing the distribution of cationic salt ions within different plant tissues (Fig. 4). Compared to the control (C0), the application of biochar significantly increased the concentration of K^+ in roots and stems by 25 to 108% and 28 to 50%, respectively. The highest accumulation (28.7 g/kg) was observed in the stems under the C3 treatment. A similar trend of increase was also noted in grains. Notably, K^+ content in both plant tissues and soil exhibited a positive correlation with biochar application rates. Conversely, although soil sodium salt content decreased, Na^+ concentrations in all plant parts increased non-significantly. Overall, Na^+ accumulation was lower in grains than in roots and stems. Regarding divalent cations, the application of biochar promoted the enrichment of Ca^{2+} and Mg^{2+} in rapeseed. Consequently, soil Ca^{2+} content increased, while soil Mg^{2+} content decreased slightly.

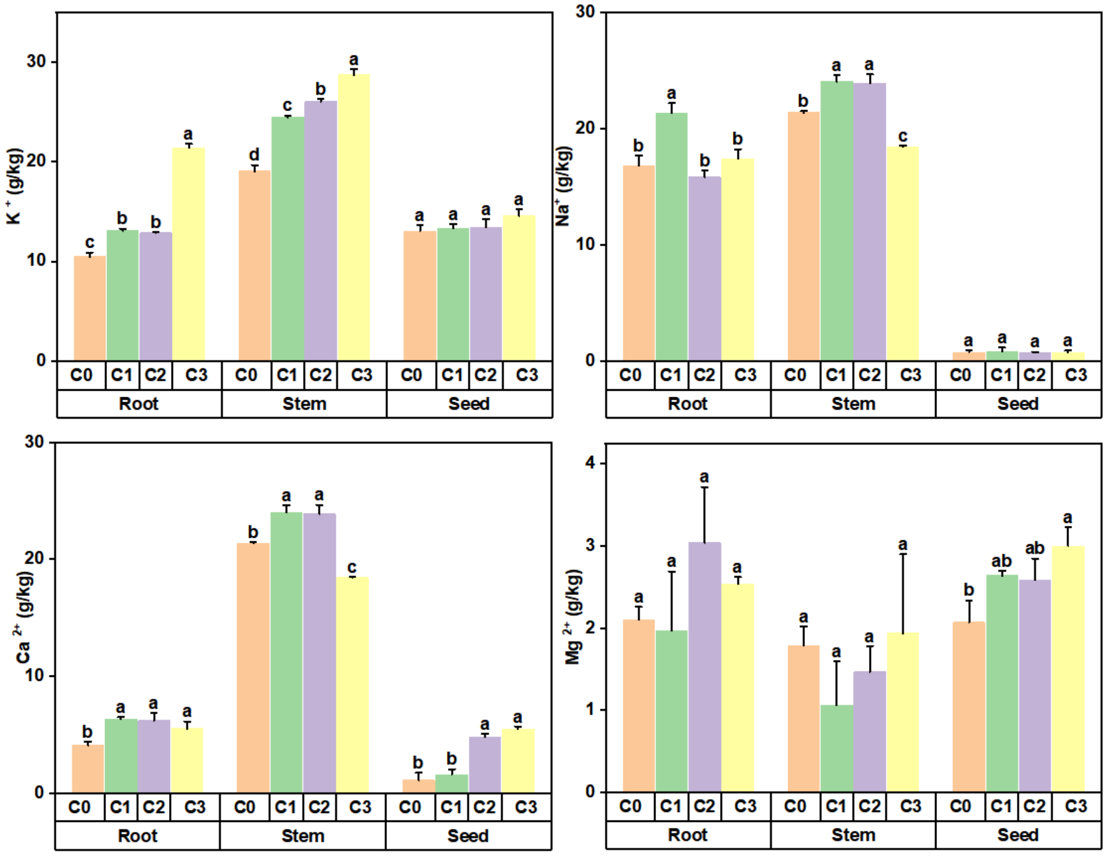

Fig. 4. Cation content in rapeseed root, stem, and seed under different biochar treatments after harvest. Biochar amendment altered the content of cationic salt ions (K^+, Na^+, Ca^{2+}, Mg^{2+}) in rapeseed tissues. Different letters indicate significant differences ($p < 0.05$) among treatments for each cation.

Effects of Biochar Amendment on Soil Microbial Biomass and Bacterial Community Dynamics

As shown in Fig. 5, the C3 treatment significantly increased the microbial biomass of carbon (MBC) and nitrogen (MBN) in the soil, primarily in large aggregates (2 to 0.2 mm). Specifically, the MBN of the C3 treatment was significantly higher than that of the control in large aggregates only, with no significant differences observed in microaggregates or fine clay particles. There were no significant changes in microbial biomass phosphorus (MBP) across all particle size fractions, although MBP values under the C3 treatment were slightly higher in large aggregates. Compared with the C0 control, the MBC, MBN and MBP content of the C1 treatment increased from 0.44 to 2.64 g/kg, 0.02 to 0.07 g/kg, and 0.11 to 0.08 (2 to 0.2 mm), respectively. There were no significant changes with C1 treatment in 0.2 to 0.075 mm and <0.075 mm soil aggregate. This significant increase in MBC and MBN in large aggregates aligns with the findings of Wang *et al*. (2021) in a double-cropping rice system, where bacterial and fungal abundances increased by 102% and 178%, respectively. This increase is attributed to the loose, porous structure of large aggregates, which facilitates sufficient contact between biochar particles and microorganisms. Notably, although the MBC:MBN and MBN:MBP ratios remained stable across treatments, the MBC:MBP ratio in the 2 to 0.2 mm aggregates was significantly higher than in other particle size fractions. This phenomenon stems from the substantial increase in MBC, while MBP did not undergo statistically significant changes, thereby elevating this ratio. This also indicates that, while biochar can alleviate limitations of nitrogen and phosphorus nutrients for soil microorganisms (Deng *et al.* 2024; Li *et al.* 2024), accumulation rates of different elements in microbial biomass vary: carbon responds most rapidly, while phosphorus lags behind. Furthermore, pot experiments by Zhu *et al*. (2022) showed that MBC and MBN were initially higher under biochar treatment, then gradually declined and stabilized. This dynamic change supports the above explanation: at the observation time point, MBC in large aggregates remained at a high level, while MBP had not yet grown in tandem, leading to a significant increase in the MBC:MBP ratio.

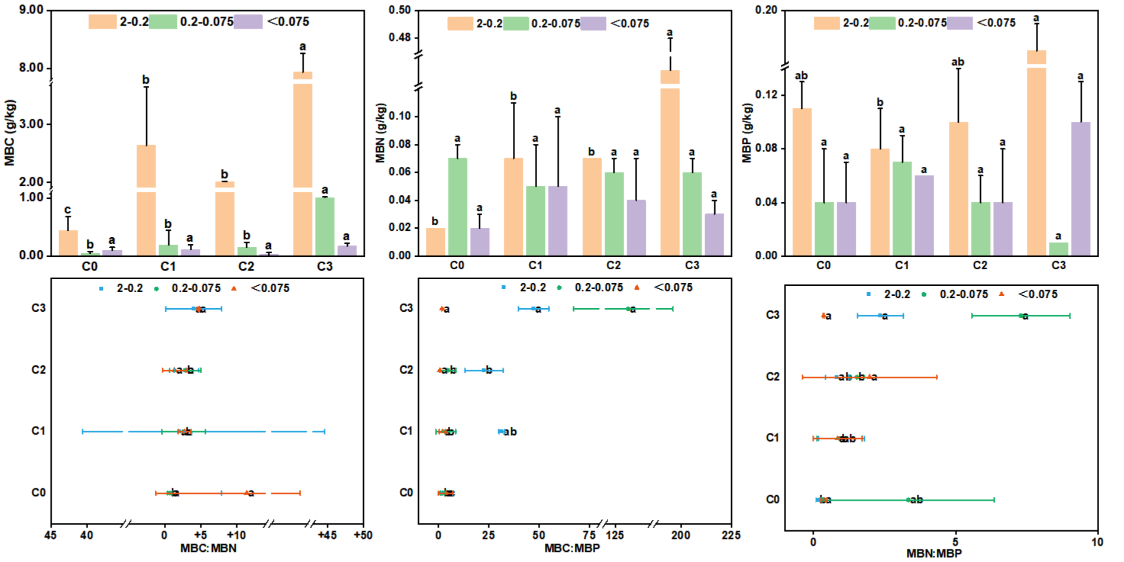

Fig. 5. Microbial biomass and stoichiometry in soil aggregates. MBC, microbial biomass carbon; MBN, microbial biomass nitrogen; MBP, microbial biomass phosphorus; MBC: MBN; MBC: MBP; and MBN: MBP. Different lowercase letters indicate statistically significant differences among treatments ($p < 0.05$ by Tukey's HSD test).

Biochar amendment significantly increased the relative abundance of dominant bacterial groups at the phylum level, including Proteobacteria, Acidobacteria, Actinobacteria, and Bacteroidetes (Fig. S2). Compared to the C0 control group, the C3 treatment exhibited the highest proportion of Proteobacteria (38.1%). In contrast, the C1 and C2 treatment groups showed the most significant increases in Acidobacteria abundance (23.3% and 23.8%, respectively), while the C3 treatment group exhibited relatively weaker effects. The high-dose biochar may inhibit this phylum. While biochar treatment generally reduced the abundance of halotolerant *Pseudomonas* species, the C3 treatment significantly increased the abundance of the halotolerant Hydrogenophilus family relative to the C0 treatment (an increase of 174.5%). This may be due to the high salinity of biochar itself, which, when applied at high doses, enhanced the abundance of halotolerant bacterial.

Biochar has been demonstrated to enhance bacterial habitats, boost bacterial activity, and increase community abundance (Heinonsalo *et al.* 2025; Zhang *et al.* 2025a). Temperature, moisture, and nutrient availability all have an effect on soil microbial communities, which are also influenced by biochar and the changes it makes to soil properties (Patel *et al.* 2021). However, biochar may contain compounds such as polycyclic aromatic hydrocarbons (PAHs), which could have a negative effect on the growth of sensitive bacterial when used in large quantities (Zhang *et al.* 2024a). Zhang *et al.* (2018) have elucidated the mechanisms by which biochar enhances the abundance of microbes in soil. Firstly, the nutrients in the biochar stimulate bacterial activity directly through synergistic metabolism and soil pretreatment effects. Secondly, the addition of biochar modifies multiple soil physicochemical properties, thereby indirectly influencing bacterial growth and activity. Thirdly, the long-term interaction between biochar and soil results in the formation of organic-mineral composite structures that enhance the capacity for water and nutrient retention, thus continuously promoting the accumulation of microbial biomass (Zhang *et al.* 2018).

Distribution of Soil Aggregate and Organic Carbon

Table S2 illustrates the effect of different rates of biochar application on the distribution of soil aggregate sizes. The results show that applying biochar significantly increases the proportion of large aggregates (>2 mm). The C2 treatment achieved a large aggregate content that was 2.93 times higher than that of the control group.

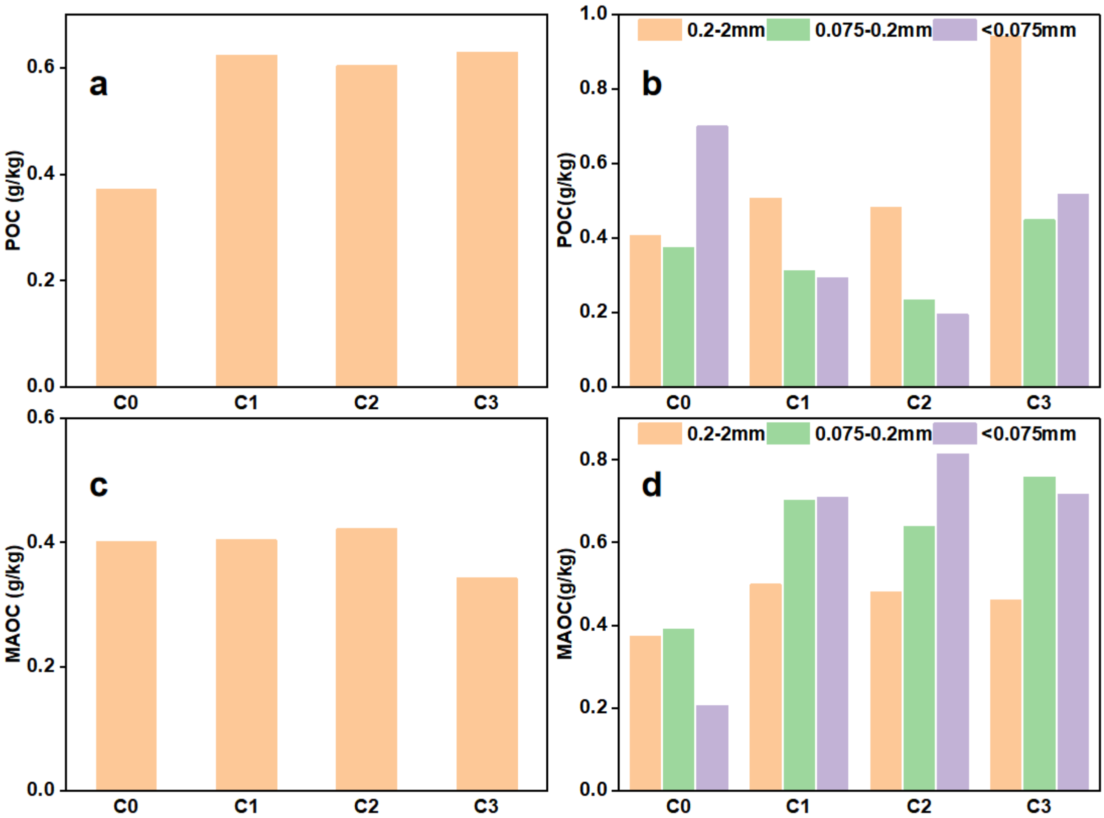

Fig. 6. Effects of biochar on the contents of soil particulate organic carbon (POC) and mineral-associated organic carbon (MOC), Unclassified (a and c); Classified (b and d). Different letters indicate significant differences ($p < 0.05$) among treatments for each cation.

The C1 and C2 treatments markedly reduced the content of small aggregates (less than 0.075 mm), whereas the C3 treatment had the opposite effect, increasing their content by 21.5%. The C2 treatment had the largest MWD and GMD, indicating the most stable aggregate structure. Overall, these results suggest that moderate biochar addition increases the proportion of large aggregates in saline-alkali soils, whereas excessive application increases the proportion of small aggregates, thereby adversely affecting aggregate stability (Yuan *et al.* 2025a).

According to the correlation analysis (Table S3), under saline-alkali soil conditions, there was no significant correlation between the application rate of biochar (BC) and any of the aggregate parameters ($p > 0.05$). This was attributed to the inhibition of biochar particle agglomeration caused by high concentrations of exchangeable Na^+ in saline-alkali soils (Lei *et al*. 2025). MWD showed a significant positive correlation with the >2 mm and 2 to 0.2 mm particle size fractions ($r = 0.719$ and 0.756, respectively), while GMD exhibited a significant positive correlation with the 2 to 0.2 mm fraction ($r = 0.732$) and a highly significant negative correlation with microaggregates <0.075 mm ($r = -0.898$). An increased proportion of large and medium aggregates improved the stability of saline-alkali soil aggregates, whereas an increase in microaggregates significantly reduced structural stability. MWD showed a highly significant positive correlation with GMD ($r = 0.857$), indicating a high degree of consistency in evaluating stability between the two. Therefore, promoting the formation of water-stable aggregates >0.2 mm was key to improving the structure of saline-alkali soils.

Prolonged agitation may cause some biochar particles larger than 53 μm to break down, which can lead to an underestimation of POC and an overestimation of MAOC. Nonetheless, biochar application in this study still significantly increased TOC and POC concentrations. Compared with the control, the greatest POC increase was observed under the C1 treatment (68%), while MAOC content decreased from 0.685 g/kg in the C0 treatment to 0.461 g/kg in the C3 treatment. The increase in POC was primarily attributed to aggregates in the 2 to 0.02 mm size fraction, with POC in this size fraction increasing significantly by 36.6% under the C3 treatment. The biochar was rich in aromatic carbon structures, such as polycyclic aromatic hydrocarbons, and had a larger particle size (>53 μm), which directly promoted the formation of POC components (Yang *et al.* 2025a). In summary, while the wet sieving process caused compositional migration between POC and MAOC, the relative differences between treatments were clear and the POC-enriching and MAOC-diluting effects of biochar were reliable.

CONCLUSIONS

1. Biochar alleviated salt stress in saline-alkali soils by increasing key nutrients (nitrogen, phosphorus, potassium) and optimizing soil microstructure.
2. Biochar significantly raised total organic carbon (TOC) levels, mainly within 2 to 0.02 mm aggregates, while reducing micro-active organic carbon for greater stability.
3. Biochar increased particulate organic carbon (POC) and mineral-associated organic carbon (MAOC) in different soil aggregates and probably can be regarded as an effective carbon sequestration practice.
4. Moderate biochar application (2%, w:w) offered a sustainable approach to enhance fertility, regulate salinity, and promoted carbon sequestration in saline-alkali lands in this study.

ACKNOWLEDGEMENTS

This work was supported by the Natural Science Foundation of Jiangsu Province [grant number BK20221407], and the Postgraduate Research and Practice Innovation Program of Yancheng Institute of Technology (KYCX24-XZ023).

Authorship Contribution

Fengli Cheng: Investigation, Writing-original draft preparation; **Guixiang Quan**: Writing-editing, Conceptualization; **Hui Wang**: Data curation; Formal analysis, **Liqiang Cui:** Software, Methodology; **Dezhi Yan**: Software; **Jinlong Yan**: Writing-reviewing, Validation, Resources.

Declaration of Competing Interest

The authors declare that they have no known competing financial interests or personal relationships that could have appeared to influence the work reported in this paper.

Data Availability Statement

The data that support the findings of this study are available from the corresponding author upon reasonable request.

REFERENCES CITED

Abiven, S., Menasseri, S., and Chenu, C. (2009). "The effects of organic inputs over time on soil aggregate stability – A literature analysis," *Soil Biology and Biochemistry* 41(1), 1-12. https://doi.org/10.1016/j.soilbio.2008.09.015

Ait Lahssaine, I., Kabiri, L., Messaoudi, B., El Hafyani, M., Essafraoui, B., Kretzschmar, H., Kurz, E., Hellriegel, U., and Hoinkis, J. (2025). "Performance assessment of 14 soil salinity spectral indices in a drought oasis environment: Rheris Oasis, Southeastern Morocco," *Scientific African* 29, e02822. https://doi.org/10.1016/j.sciaf.2025.e02822

Bao, S. (2008). *Soil Agricultural Chemical Analysis*, 3rd Ed., China Agriculture Press, China.

Chen, H., He, Y., Wang, X., Luo, S., Jiao, Y., and Han, S. (2024). "Mapping China's reserved arable lands and its sustainable cropping layout," *Journal of the Science of Food and Agriculture* 104(15), 9180-9190. https://doi.org/10.1002/jsfa.13739

Cui, L., Liu, Y., Yan, J., Hina, K., Hussain, Q., Qiu, T., and Zhu, J. (2022). "Revitalizing coastal saline-alkali soil with biochar application for improved crop growth," *Ecological Engineering* 179: 106594. https://doi.org/10.1016/j.ecoleng.2022.106594

Cui, L., Pan, G., Li, L., Bian, R., Liu, X., Yan, J., Quan, G., Ding, C., Chen, T., Liu, Y., Liu, Y., Yin, C., Wei, C., Yang, Y., and Hussain, Q. (2016). "Continuous immobilization of cadmium and lead in biochar amended contaminated paddy soil: A five-year field experiment," *Ecological Engineering* 93, 1-8. https://doi.org/10.1016/j.ecoleng.2016.05.007

Defaix, C., Aymes, A., Albe Slabi, S., Basselin, M., Mathé, C., Galet, O., and Kapel, R. (2019). "A new size-exclusion chromatography method for fast rapeseed albumin and globulin quantification," *Food Chemistry* 287, 151-159. https://doi.org/10.1016/j.foodchem.2019.01.209

Deng, L., Tu, P., Ahmed, N., Zhang, G., Cen, Y., Huang, B., Deng, L., and Yuan, H. (2024). "Biochar-based phosphate fertilizer improve phosphorus bioavailability, microbial functioning, and citrus seedling growth," *Scientia Horticulturae* 338, 113699. https://doi.org/10.1016/j.scienta.2024.113699

dos Santos, W., Gonzaga, M., da Silva, A., and de Almeida, A. (2022). "Improved water and ions dynamics in a clayey soil amended with different types of agro-industrial waste biochar," *Soil and Tillage Research* 223, 105482. https://doi.org/10.1016/j.still.2022.105482

Duan, M., Liu, G., Zhou, B., Chen, X., Wang, Q., Zhu, H., and Li, Z. (2021). "Effects of modified biochar on water and salt distribution and water-stable macro-aggregates in saline-alkaline soil," *Journal of Soils and Sediments* 21(6), 2192-2202. https://doi.org/10.1007/s11368-021-02913-2

Feng, Q., Wang, B., Zimmerman, A. R., Wu, P., Lee, X., Chen, M., and Zhang, J. (2024). "Application of C and N isotopes to the study of biochar biogeochemical behavior in soil: A review," *Earth-Science Reviews* 256, 104860. https://doi.org/10.1016/j.earscirev.2024.104860

Haj Amor, Z., Araya, T., Kim, D. G., Bouri, S., Lee, J., Ghiloufi, W., Yang, Y., Kang, H., Jhariya, M.K., Banerjee, A., and Lal, R. (2022). "Soil salinity and its associated effects on soil microorganisms, greenhouse gas emissions, crop yield, biodiversity and desertification: A review," *Science of The Total Environment* 843, 156946. https://doi.org/10.1016/j.scitotenv.2022.156946

Heinonsalo, J., Peltokangas, K., Barré, P., Baudin, F., Cécillon, L., Kalu, S., Kanerva, S., Karhu, K., Kulmala, L., Liski, J., Salonen, A., Shrestha, R., Soinne, H., Virtanen, E., Huusko, K., and Sietiö, O. M. (2025). "Effects of biochar, ligneous soil amendments, and a microbial stimulant on soil biological activity, and carbon content and stability after two-years of their application in a boreal cropland," *Heliyon* 11(12), e43536. https://doi.org/10.1016/j.heliyon.2025.e43536

Jiang, W., Li, T., Ma, J., Wang, X., Cheng, Y., Gong, L., Zhang, J., and Chen, G. (2025). "Organic materials input promotes the soil aggregate sequestration through changing soil aggregates structure and stability," *Journal of Environmental Management* 393, 127027. https://doi.org/https://doi.org/10.1016/j.jenvman.2025.127027

Jeffery, S., Verheijen, F., van der Velde, M., and Bastos, A. (2011). "A quantitative review of the effects of biochar application to soils on crop productivity using meta-analysis," *Agriculture, Ecosystems and Environment* 144(1), 175-187. https://doi.org/10.1016/j.agee.2011.08.015

Ju, W., Sardans, J., Bing, H., Wang, J., Ma, D., Cui, Y., Duan, C., Li, X., Fan, Q., Peñuelas, J., and Fang, L. (2024). "Diversified vegetation cover alleviates microbial resource limitations within soil aggregates in tailings," *Environmental Science and Technology* 58(42), 18744-18755. https://doi.org/10.1021/acs.est.4c06081

Lehmann, J., Kuzyakov, Y., Pan, G., and Ok, Y. (2015). "Biochars and the plant-soil interface," *Plant & Soil* 395(1-2), 1-5. https://doi.org/10.1007/s11104-015-2658-3

Lei, S., Jia, X., Zhao, C., and Shao, M. (2025). "A review of saline-alkali soil improvements in China: Efforts and their impacts on soil properties," *Agricultural Water Management* 317, 109617. https://doi.org/10.1016/j.agwat.2025.109617

Li, D., Qi, Z., Guo, J., Wang, T., Li, X., and Hou, N. (2025a). "Study on the screening of high-efficiency salt and alkali-tolerant microbial agents and their roles and mechanisms in enhancing saline-alkaline soil remediation," *Journal of Cleaner Production* 519, article 145992. https://doi.org/10.1016/j.jclepro.2025.145992

Li, H., Liu, G., Dan, C., Zhou, Z., Liu, Y., Liu, C., Shen, E., Zhang, Q., Xia, X., Liu, D., Guo, Z., and Zhao, X. (2025b). "Effects of soil porosity on water stability of aggregates," *Soil and Tillage Research* 254, 106741. https://doi.org/10.1016/j.still.2025.106741

Li, Q., Ji, H., Zhang, C., Cui, Y., Peng, C., Chang, S. X., Cao, T., Shi, M., Li, Y., Wang, X., Zhang, J., and Song, X. (2024). "Biochar amendment alleviates soil microbial nitrogen and phosphorus limitation and increases soil heterotrophic respiration under long-term nitrogen input in a subtropical forest," *Science of the Total Environment* 951, 175867. https://doi.org/10.1016/j.scitotenv.2024.175867

Liu, S., Wang, N., Li, D., Tian, C., Zhang, K., Hu, M., Niu, H., and Zhao, Z. (2024). "Effects of halophyte Suaeda salsa continuous cropping on physical and chemical properties of saline soil under drip irrigation in arid regions," *Agriculture, Ecosystems and Environment* 371, 109076. https://doi.org/10.1016/j.agee.2024.109076

Liu, Z., Chen, X., Jing, Y., Li, Q., Zhang, J., and Huang, Q. (2014). "Effects of biochar amendment on rapeseed and sweet potato yields and water stable aggregate in upland red soil," *Catena* 123, 45-51. https://doi.org/10.1016/j.catena.2014.07.005

Lu, S., Sun, F., and Zong, Y. (2014). "Effect of rice husk biochar and coal fly ash on some physical properties of expansive clayey soil (Vertisol)," *Catena* 114, 37-44. https://doi.org/10.1016/j.catena.2013.10.014

Patel, K., Fansler, S., Campbell, T., Bond-Lamberty, B., Smith, A., RoyChowdhury, T., McCue, L., Varga, T., and Bailey, V. (2021). "Soil texture and environmental conditions influence the biogeochemical responses of soils to drought and flooding," *Communications Earth and Environment* 2(1). https://doi.org/10.1038/s43247-021-00198-4

Quan, G., Fan, Q., Sun, J., Cui, L., Wang, H., Gao, B., and Yan, J. (2020a). "Characteristics of organo-mineral complexes in contaminated soils with long-term biochar application," *Journal of Hazardous Materials* 384, 121265. https://doi.org/10.1016/j.jhazmat.2019.121265

Quan, G., Fan, Q., Zimmerman, A. R., Sun, J., Cui, L., Wang, H., Gao, B., and Yan, J. (2020b). "Effects of laboratory biotic aging on the characteristics of biochar and its water-soluble organic products," *Journal of Hazardous Materials* 382, 121071. https://doi.org/10.1016/j.jhazmat.2019.121071

Schurkamp, S., Lishawa, S., and Ohsowski, B. (2024). "Wetland plant species and biochar amendments lead to variable salinity reduction in roadway-associated soils," *Science of the Total Environment* 951, article 175801. https://doi.org/10.1016/j.scitotenv.2024.175801

Simiele, M., Argentino, O., Baronti, S., Scippa, G. S., Chiatante, D., Terzaghi, M., and Montagnoli, A. (2022). "Biochar enhances plant growth, fruit yield, and antioxidant content of cherry tomato (*Solanum lycopersicum* L.) in a soilless substrate," *Agriculture* 12(8), 1135. https://doi.org/10.3390/agriculture12081135

Wang, C., Chen, D., Shen, J., Yuan, Q., Fan, F., Wei, W., Li Y., and Wu, J. (2021). "Biochar alters soil microbial communities and potential functions 3–4 years after amendment in a double rice cropping system," *Agriculture, Ecosystems & Environment* 311, 107291. https://doi.org/https://doi.org/10.1016/j.agee.2020.107291

Wang, S., Wang, J., Dong, G., Chen, X., Wang, S., Lei, F., Su, X., and Bai, Q. (2022). "Effect of different extraction methods on quality characteristics of rapeseed and flaxseed oils," *Journal of Food Quality* 2022, 1-12. https://doi.org/10.1155/2022/8296212

Wang, M., Zhu, Y., Yue, C., Ge, H., Yan, J., Yang, Y., and Quan, G. (2024a). "Preparation of a novel magnetic calcium-based biochar for arsenic removal: Behavior and dominant mechanism," *Separation and Purification Technology* 336, article 126384. https://doi.org/10.1016/j.seppur.2024.126384

Wang, X., Riaz, M., Babar, S., Eldesouki, Z., Liu, B., Xia, H., Li, Y., Wang, J., Xia, X., and Jiang, C. (2024b). "Alterations in the composition and metabolite profiles of the saline-alkali soil microbial community through biochar application," *Journal of Environmental Management* 352, 120033. https://doi.org/10.1016/j.jenvman.2024.120033

Wang, J., Sun, L., Sun, Y., Yang, S., Qin, Q., and Xue, Y. (2025a). "Long-term biochar-based fertilizer substitution promotes carbon, nitrogen, and phosphorus acquisition enzymes in dryland soils by affecting soil properties and regulating bacterial community," *Applied Soil Ecology* 206, 105801. https://doi.org/10.1016/j.apsoil.2024.105801

Wang, Z., Liu, X., Han, J., Xu, B., Ma, W., Lu, Y., and Ye, X. (2025b). "Effects of long-term biochar addition on the wheat-rotated rice grain yield and the fate of N fertilizer in plant-soil system—A combined 15N study," *European Journal of Agronomy* 168, 127645. https://doi.org/10.1016/j.eja.2025.127645

Wu, J., Zhou, B., Li, Z., Liu, C., Li, Y., Wang, Y., Zhao, N., Wang, Z., Chai, Y., Scopa, A., Drosos, M., Rajput, V., and Shan, S. (2025). "Biochar promoted soil organic carbon accumulation and aggregate stability by increasing the content of organic complex metal oxides in paddy soil," *Soil and Tillage Research* 254, 106713. https://doi.org/10.1016/j.still.2025.106713

Wu, Q., Chen, Y., Dou, X., Liao, D., Li, K., An, C., Li, G., and Dong, Z. (2024). "Microbial fertilizers improve soil quality and crop yield in coastal saline soils by regulating soil bacterial and fungal community structure," *Science of the Total Environment* 949, 175127. https://doi.org/10.1016/j.scitotenv.2024.175127

Xie, L., Ma, Q., Chen, Q., Liu, Y., Guo, P., Zhang, J., Duan, G., Lin, A., Zhang, T., and Li, S. (2025). "Efficient remediation of different concentrations of Cr-contaminated soils by nano zero-valent iron modified with carboxymethyl cellulose and biochar," *Journal of Environmental Sciences* 147, 474-486. https://doi.org/10.1016/j.jes.2023.12.007

Yang, C., Chang, Y., Liu, J., Tian, Y., Lu, S., and Wang, J. (2025a). "Differences in the physical protection mechanisms of soil organic carbon with 13C-labeled straw and biochar," *Biochar* 7(1), article 32. https://doi.org/10.1007/s42773-025-00430-w

Yang, X., Wong, S., Ge, L., Chan, W., and Lisak, G. (2025b). "Enhancing vegetable yield and quality in urban farming under soil and soil-less conditions: The synergistic role of biochar in food security and waste management," *Journal of Cleaner Production* 513, 145724. https://doi.org/10.1016/j.jclepro.2025.145724

Yuan, H., Wu, Y., Sun, Y., Liu, J., Lin, L., Xia, F., Su, X., Sun, Q., and Meng, J. (2025a). "Differential effects of biochar and straw incorporation on soil organic carbon: A case study on paddy cultivation in Northeast China," *Journal of Environmental Management* 390, 126284. https://doi.org/10.1016/j.jenvman.2025.126284

Yuan, H., Zhang, Z., Li, M., Clough, T., Wrage-Mönnig, N., Qin, S., Ge, T., Liao, H., and Zhou, S. (2019). "Biochar's role as an electron shuttle for mediating soil N_2O emissions," *Soil Biology and Biochemistry* 133, 94-96. https://doi.org/10.1016/j.soilbio.2019.03.002

Yuan, X., Ban, G., Luo, Y., Wang, J., Peng, D., Liang, R., He, T., and Wang, Z. (2025b). "Biochar effects on aggregation and carbon-nitrogen retention in different-sized aggregates of clay and loam soils: A meta-analysis," *Soil and*

Tillage Research 247, 106365. https://doi.org/10.1016/j.still.2024.106365
Yue, Y., Lin, Q., Li, G., Zhao, X., and Chen, H. (2023). "Biochar amends saline soil and enhances maize growth: Three-year field experiment findings," *Agronomy* 13(4), article 1111. https://doi.org/10.3390/agronomy13041111
Zamani, S., Arminian, A., Zarei, B., and Hajinia, S. (2025). "The impact of drought stress on morpho-physiological characteristics of rapeseed cultivars (*Brassica napus* L.)," *Oil Crop Science* 10(2), 165-176. https://doi.org/10.1016/j.ocsci.2025.04.004
Zhang, C., Li, Z., Miao, Y., and Liao, X. (2025a). "Combining effects of nitrogen fertilizer and biochar on soil N_2O emissions and microbial community in a subtropical rapeseed-soybean rotation," *European Journal of Soil Biology* 126, 103750. https://doi.org/10.1016/j.ejsobi.2025.103750
Zhang, J., Wang, Y., Shi, Y., Yang, B., Zhang, A., Du, Z., Zhong, G., Luo, C., Zhang, G., and Wang, J. (2024a). "Dosage- and site-dependent retention of black carbon and polycyclic aromatic hydrocarbons in farmland soils via long-term biochar addition," *Carbon Research* 3(1), article 14. https://doi.org/10.1007/s44246-023-00095-9
Zhang, L., Jing, Y., Xiang, Y., Zhang, R., and Lu, H. (2018). "Responses of soil microbial community structure changes and activities to biochar addition: A meta-analysis," *Science of the Total Environment* 643, 926-935. https://doi.org/10.1016/j.scitotenv.2018.06.231
Zhang, W., Munkholm, L., Heck, R., Watts, C., and Jensen, J. (2025b). "Aggregate pore and shape properties were more strongly correlated to soil organic carbon in large aggregates: Evidence from a long-term management-induced soil carbon gradient," *Geoderma* 459, 117357. https://doi.org/10.1016/j.geoderma.2025.117357
Zhang, Y., Miao, S., Song, Y., Wang, X., and Jin, F. (2024b). "Biochar application reduces saline–alkali stress by improving soil functions and regulating the diversity and abundance of soil bacterial community in highly saline–alkali paddy field," *Sustainability* 16(3), 1001. https://doi.org/10.3390/su16031001
Zhao, S., Wang, X., Wang, Q., Sumpradit, T., Khan, A., Zhou, J., Salama, E., Li, X., and Qu, J. (2023). "Application of biochar in microbial fuel cells: Characteristic performances, electron-transfer mechanism, and environmental and economic assessments," *Ecotoxicology and Environmental Safety* 267, 115643. https://doi.org/10.1016/j.ecoenv.2023.115643
Zhu, L., Tian, G., Zhang, L., Zhao, X., Wang, J., Wang, C., Wang, P., and Tian, E. (2022). "Biochar application affects dynamics of soil microbial biomass and maize grain yield," *ScienceAsia* 48(5), 673. https://doi.org/10.2306/scienceasia1513-1874.2022.101
Zou, W., Lang, M., Zhang, L., Liu, B., and Chen, X. (2022). "Ammonia-oxidizing bacteria rather than ammonia-oxidizing archaea dominate nitrification in a nitrogen-fertilized calcareous soil," *Science of the Total Environment* 811, 151402. https://doi.org/10.1016/j.scitotenv.2021.151402

Article submitted: March 16, 2026; Peer review completed: April 4, 2026; Revised version received and accepted: May 27, 2026; Published: June 10, 2026.
DOI: 10.15376/biores.21.3.6846-6865

SUPPLEMENTARY MATERIALS

Determination of TOC and TN

Total organic carbon (TOC) was determined using the potassium dichromate external heating method. Place 0.1 g of 100-mesh soil in a 250 mL conical flask, and add 5 mL of 0.8 mol/L potassium dichromate solution and 5 mL of concentrated sulphonic acid. Digest at 170 to 180 °C in an electric furnace for 5 min. Cool the flask and rinse the inner walls with distilled water to maintain a solution volume of 60 to 70 mL. Add 2 to 3 drops of o-phenanthroline indicator and titrate with 0.2 mol/L ferrous sulphate solution, while recording the endpoint volume. Total soil nitrogen (TN) was determined using the semi-micro Kjeldahl method. Weigh a 1 g sample of soil (100 mesh) and add 5 mL of concentrated sulphonic acid and 2 g of mixed catalyst (potassium sulphate, copper sulphate, and selenium powder in a ratio of 100:10:1), and digest the sample on an electric hotplate. Once digested, cool and distil it using a Kjeldahl nitrogen analyzer (KDN-520). Titrate with 0.01 mol/L hydrochloric acid until the endpoint is reached. Add 10 g of soil and 50 mL of distilled water, soak for three min, followed by vacuum filtration. Measure the total salt content of the soil by weighing the dried residue.

Table S1. Soil and Biochar Properties

	Soil	BC
pH	7.97±0.05	9.43±0.04
TOC(g/kg)	3.53±0.10	528.60±76.89
TK(g/kg)	3.59 ±0.07	5.23±0.06
TP(g/kg)	0.74±0.01	3.79±1.01
TN(g/kg)	0.26±0.06	3.10±0.52
Capacity(g/cm^3)	1.80±0.00	-
Total soil salinity (g/kg)	1.525±0.247	7.155±0.750
K^+ (g/kg)	0.181±0.025	2.030±0.006
Na^+ (g/kg)	0.673±0.062	0.809±0.006
Ca^{2+} (g/kg)	0.454±0.057	0.104±0.083
Mg^{2+} (g/kg)	0.061±0.001	0.005±0.002

Notes: TOC, soil organic carbon; TK, Total soil potassium; TP, total soil phosphorus; TN, Total soil nitrogen; K^+, Soil water-soluble K; Na^+, Soil water-soluble Na; Ca^{2+}, Soil water-soluble Ca; Mg^{2+}, Soil water-soluble Mg. Values are means ± SD.

Table S2. Mass Percentage of Soil Microaggregates under Different Biochar Treatments and Soil Aggregate Stability

	3-2mm (%)	2-0.2mm (%)	0.2-0.075mm (%)	＜0.075mm (%)	MWD (mm)	GMD (mm)
C0	0.044	0.356	0.339	0.260	0.5583	0.2345
C1	0.066	0.397	0.372	0.165	0.6594	0.3064
C2	0.129	0.347	0.344	0.179	0.7585	0.3273
C3	0.063	0.257	0.364	0.316	0.5024	0.1873

Table S3. Correlation between Biochar with MWD, GMD and Particle Size

	BC	**MWD**	**GMD**	**＞2mm**	**2-0.2mm**	**0.2-0.075mm**	**＜0.075mm**
BC	1						
MWD	-0.293	1					
GMD	-0.293	0.857**	1				
＞2mm	0.417	0.719*	0.539	1			
2-0.2mm	-0.65	0.756*	0.732*	0.184	1		
0.2-0.075mm	0.146	-0.619	-0.31	-0.395	-0.659	1	
＜0.075mm	0.393	-0.587	-.898**	-0.181	-0.638	0.036	1

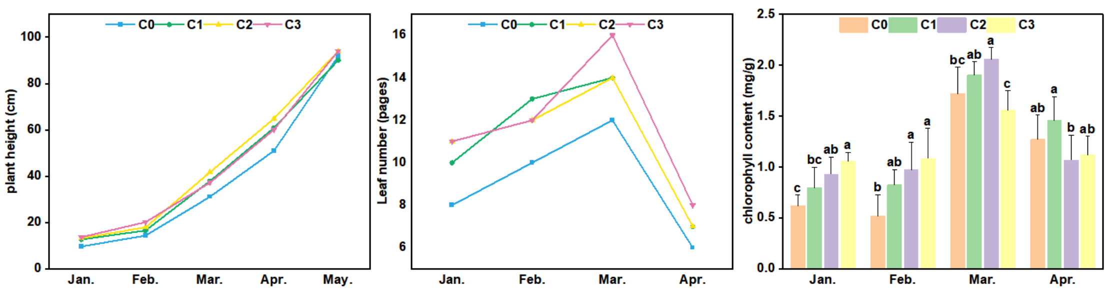

Fig. S1. Effect of different biochar treatments on plant height, number of leaves and leaf chlorophyll in plants. Different lowercase letters indicate statistically significant differences among treatments ($p < 0.05$ by Tukey's HSD test).

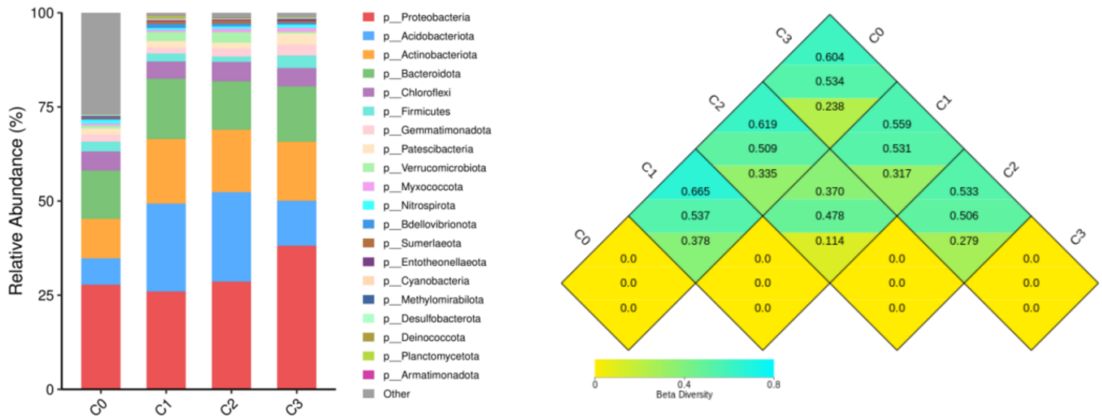

Fig. S2. Heat map of bacterial community structure and diversity indices at each treatment gate level